Instrument Science Report WFC3 2015-12

WFC3/UVIS Shutter Characterization

Kailash Sahu, C.M. Gosmeyer, Sylvia Baggett
July 08, 2015

ABSTRACT

A series of internal flat field images and standard star observations were obtained to check the shutter performance. The series of images were similar to the ones taken during SMOV so that the performance of the shutter could be compared with the performance during SMOV in 2009, and check if the behavior of shutter mechanism has changed in the meantime. The flat field images show that the intensity of the flat field lamp has decreased by about 1.6 +/- 0.2% over the past 6 years. Our observations are consistent with the earlier finding that the variation in exposure time across the detector due to shutter shading is less than 0.1%. The standard star observations show that there is no noticeable difference in the present performance of the shutter mechanism compared to its performance during SMOV.

1. Introduction

The WFC3 shutter-wheel mechanism is described in detail in several reports (e.g. WFC3 Handbook; Hilbert 2009; Sahu, Baggett and MacKenty, 2014; Hartig, 2008); the essential points are repeated here for completeness. The WFC3 shutter mechanism is essentially a circle divided into four quadrants (Fig. 1). Two of the quadrants are clear and two are closed. While the shutter motor is capable of moving the shutter wheel in either the clockwise or counter clockwise direction, the operations software limits the shutter motion to the clockwise (as seen down the beam and onto the detector) direction only. In UVIS images, the shutter blade advances from the corner of amplifier D in the lower right corner, up to the corner of amplifier A in the upper left corner of the detector.

When the shutter is in the closed position, a commanded move of 90° places it into an

open configuration. At the end of an exposure, another move of 90° places the shutter back into a closed position. For all commanded exposure times longer than 0.48 seconds, the shutter blade rotates out of the beam, stays in the open position for the commanded exposure time, and then rotates in the same direction until the opposite shutter blade intercepts the beam, closing the shutter. For the minimum commanded exposure time of 0.48 seconds, the shutter does not stop its rotation during the exposure (Hilbert, 2009).

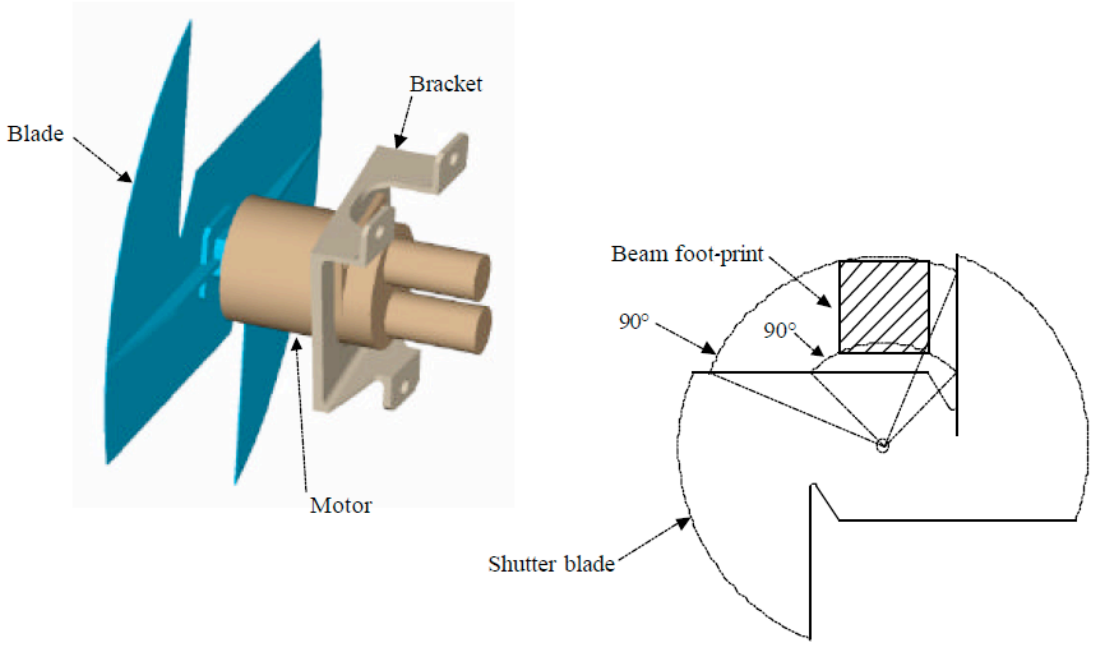

Figure 1: Graphical representation of the UVIS shutter mechanism, reproduced from the WFC3 OP-01 document (Baggett 2003)

The first goal of the current program (14019) was to check possible shutter shading effects on the detector. If the shutter wheel were to move at a non-uniform velocity when opening or closing, the result would be a non-uniform exposure time across the detector, also known as shutter shading. The tests conducted during SMOV had shown that any exposure time variation caused by the shutter shading effect is less than 0.1% (Hilbert, 2009). Our goal was to repeat some of the observations and compare with the SMOV results. The second goal was to examine the shutter timing accuracy. For a commanded exposure time, our goal was to measure the actual amount of time the detector was exposed to the beam. Finally, we wanted to investigate the repeatability of the shutter. For a set of images commanded to have identical exposure times, we measured the flux collected in each image to look for consistency.

2. Observations

Observations were made in two separate Visits. During the first Visit, we collected 6 full-

frame internal flat fields (illumination provided by the Tungsten lamp) with exposure times ranging from 0.5 seconds up to 17 seconds. In Visits 2, we collected a set of observations similar to the observations taken during SMOV, of the standard star GD153 through the F395N filter. Exposure times varied from 0.5 to 30 seconds. F395N was chosen in order to avoid saturation in the longer exposures, but still achieve good signal-to-noise values of GD153 for the shorter of exposure times, enabling good measurements of shutter timing and repeatability. The target was placed in the C amp (lower left quadrant) and the UVIS2-C512C-SUB subarray used, where only the C amp was read out. Exposure times were arranged in random order, rather than monotonically increasing or decreasing.

3. Data Reduction

In order to carry out a comparative analysis of the SMOV data (Prog. 11427) and the current data (Prog. 14019), we processed all the data from both the programs in a consistent manner. All files were reduced with the CALWF3 pipeline. The flat fields acquired in the first visit of both programs had the overscan pixel-derived bias level subtracted, along with bias and dark current images subtracted. These steps, along with a flat field correction, were performed on the standard star observations in the Visit 2 data of both programs. Since the CTE effect was negligible during SMOV, which has since increased significantly, we applied CTE correction algorithm to only the observations taken for program 14019.

4. Analysis

Flat Field Images:
If the UVIS shutter rotates with a variable speed, pixels across the detector will experience a non-uniform exposure time. For example, if the shutter blade for a 0.5s exposure were to begin rotating at a given speed and then slowly accelerate up to some terminal speed as it uncovered the detector, the area of the detector uncovered first will have a longer exposure time than the area uncovered last. If present, this effect would be visible as a large scale variation in brightness from the corner of the detector towards the center, as this is the direction of the shutter blade movement relative to the detector.

We examined the counts from the flat-field images at different parts of the detector, for the SMOV as well as the current program. The actual counts observed for the two programs in different areas of the detector are shown in Table 1. Hilbert (2009) used the SMOV data to investigate the shading effect (WFC3 ISR 2009-25) and concluded that the variation in exposure time due to any shading effect is less than 0.1%. We compared the two datasets (11427 and 14019), which led to the following results.

(i) The countrates in the flat-field images taken for program 14019 are lower by about 1.6 +/- 0.2% compared to the SMOV data (as shown in Fig. 2).

(ii) The relative counts at different parts of the detector are identical to the counts observed during SMOV (except for the decrease of 1.4 to 1.6%), and thus consistent with shutter shading effects of less than 0.1%.

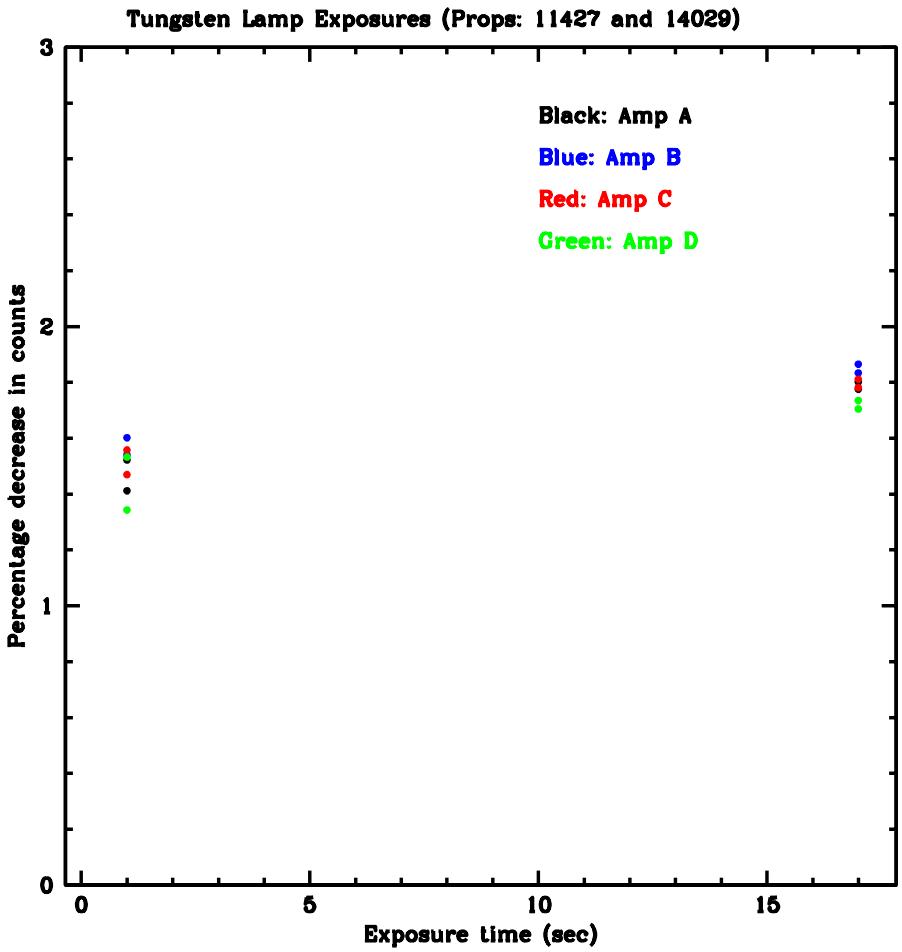

Fig. 2. The percentage decrease in counts during the past ~6 years is shown on the y-axis (represented by [(Counts(11427) - Counts(14019))*100] / [(Counts(11427) + Counts(14019))/2]) as a function of the exposure time. Average counts in 14019 are lower by 1.4 to 1.8% compared to 11427. The blade used (A or B) has no noticeable effect on the counts.

The decrease in the count rates in the 14019 flat-field images as described above suggests that the intensity of the tungsten lamp has decreased by about 1.6+/-0.2% over the past 6 years (corresponding to ~0.25% per year), which is consistent with what is observed in other data (Bourque and Baggett, 2015).

Table 1: Observed counts in different amplifiers

Filename	Shut-ter	Exp. time (s)	Av. Counts (A)	Av. Counts (B)	Av. Counts (C)	Av. Counts (D)
Program: 11427						
iaai01rqq_flt	A	0.48	813.	958.3	943.9	1155.4
iaai01rrq_flt	B	0.48	834.3	981.6	967.5	1184.6
iaai01rtq_flt	A	1.00	1734.6	2044.0	2013.5	2464.2
iaai01ruq_flt	B	1.00	1730.2	2039.0	2008.0	2459.3
iaai01rwq_flt	A	17.00	29655.4	35020.6	34679.4	42286.3
iaai01rxq_flt	B	17.00	29657.3	35022.6	34682.7	42290.5
Program 14019:						
icr401kbq_flt	B	0.48	797.4	938.5	924.8	1134.2
icr401kcq_flt	A	0.48	817.1	962.1	948.5	1162.0
icr401keq_flt	B	1.00	1704.1	2006.6	1976.9	2421.8
icr401kfq_flt	A	1.00	1710.3	2012.7	1984.2	2431.3
icr401khq_flt	B	17.00	29127.7	34375.3	34060.1	41563.1
icr401kiq_flt	A	17.00	29133.6	34384.2	34067.3	41571.6

Comparison with Bowtie Flat Fields

A program routinely run on-orbit to monitor for QE hysteresis effects acquires 1-sec internal flatfield exposures (Bourque & Baggett, 2015). The bowtie flatfields are 3x3 binned exposures, potentially useful for time-evolution studies precisely because they are taken so frequently. For the purposes of this study, the 1 sec exposure time may already be long enough that any shutter anomalies will be washed out; however, given the availability of the flatfields in the archive, they have been analyzed for any evidence of shutter changes.

The flatfields are first median-filtered in order to smooth out the high-frequency structures due to dust on the CCD window and filter; then image statistics are measured in the four corners near the amplifiers. To factor out any longterm changes of the lamp

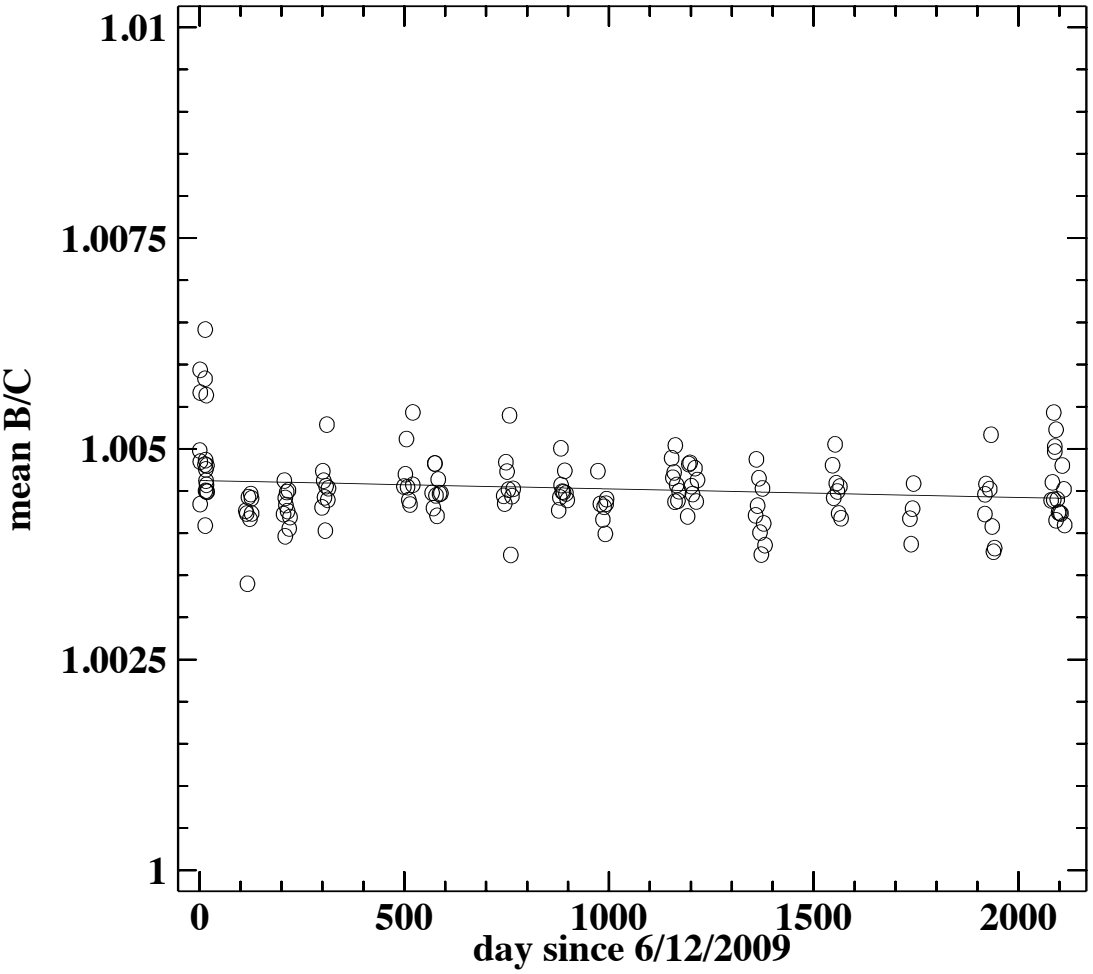

Fig. 3. Flux ratio from B and C amplifiers as observed in the bowtie monitoring data.

output flux, ratios are formed between the diametrically-opposed amps of a given image (amp B to amp C, and amp A to amp D). Since the shutter blade sweeps across the WFC3 FOV from amp D to A, with pivot point roughly outside of amp B, presumably any changes in shutter speed over the years will manifest as a trend in the A/D ratios over time. However, no significant trend in amp ratio was found; the slopes were ~1e-07/day for both B/C (see Fig. 3) and A/D (see Fig. 4). This further confirms that the shutter shading effect has not changed over the past ~7 years.

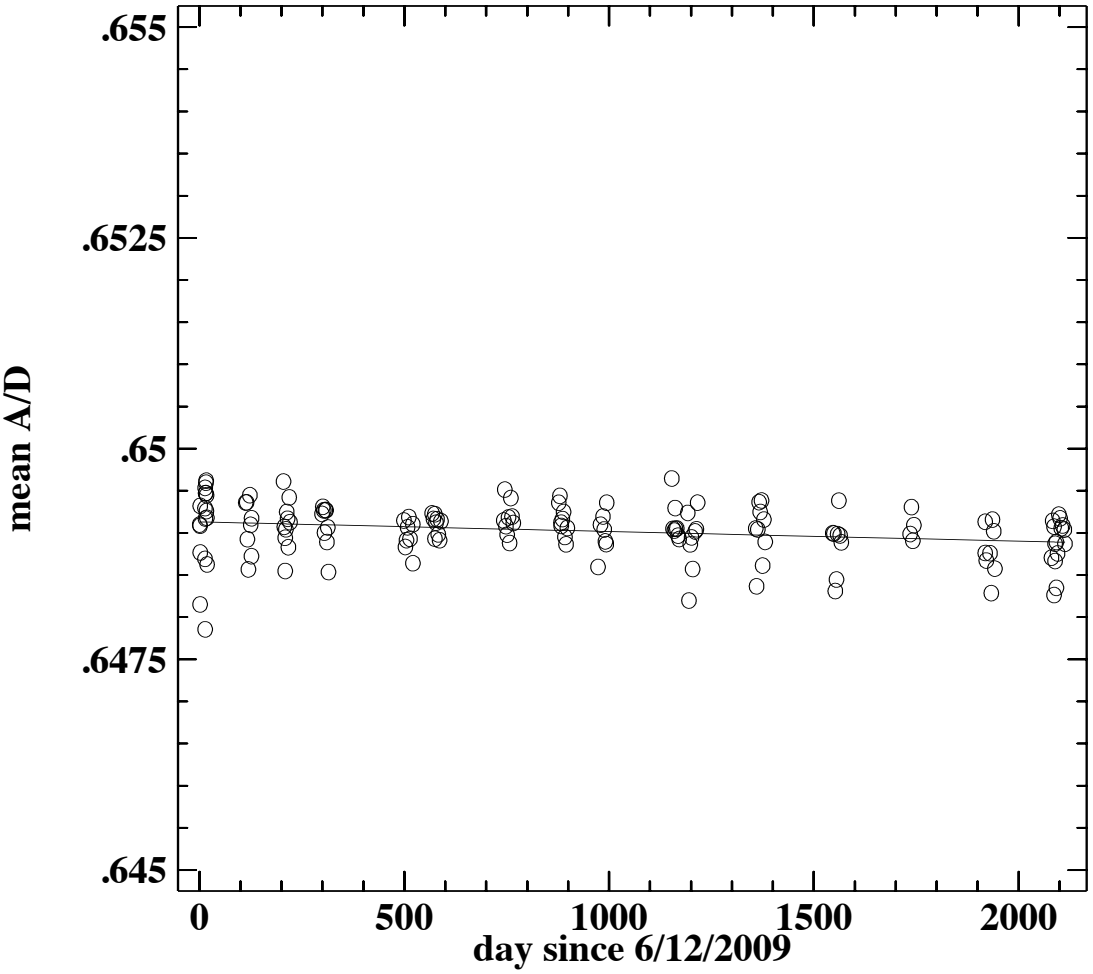

Fig. 4. Flux ratio from A and D amplifiers as observed in the bowtie monitoring data.

Photometry of the standard star:

To carry out the photometry of the standard star, the FLT images were used for program 11427, and the CTE-corrected FLC images were used for 14019. In each program, several exposures were taken with exposure times of 0.48, 0.695, 0.8, 1.0 and 30.0 seconds. Fig. 5 shows the photometric magnitudes averaged over all the images for each exposure time. The photometry is consistent in all the exposures, which suggests that the effect of shutter speed is not significant. This is further confirmed by Fig. 6 and 7, which show the photometric results from individual images. In Fig. 6 we plot the photometry for different exposure times in separate bins. The derived photometric values are consistent in all exposure times. In Fig. 7, we plot the individual measurements for different exposure times in different colors. Again, the photometry is consistent in all exposures, and does not show any time evolution. However, the photometric accuracy in the shortest exposures (<1 sec) is >0.015 magnitudes, and higher S/N observations in all exposures are necessary to investigate this effect in more detail. In an upcoming visit, we plan to observe a field containing a combination of bright and faint stars so that we have high S/N both in short as well as long exposures.

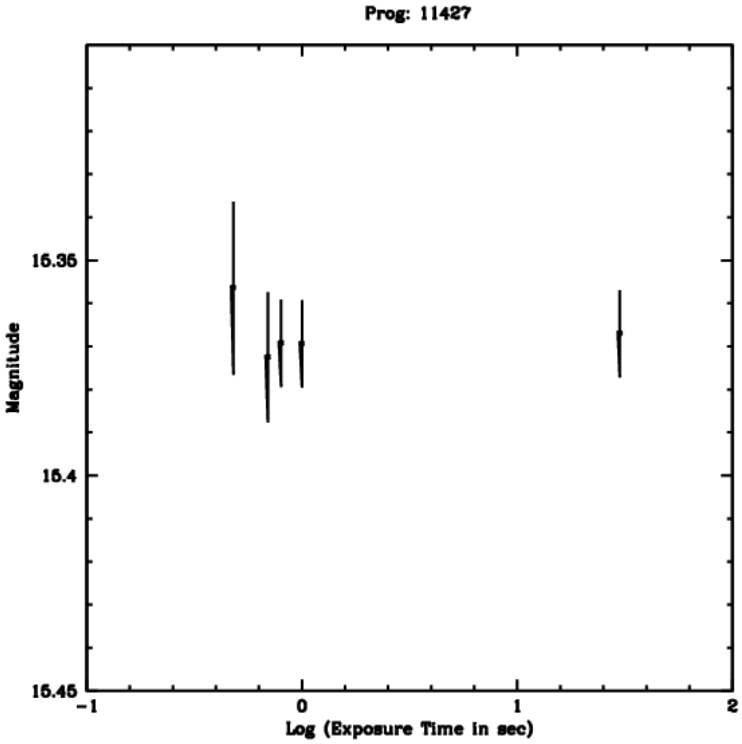

Fig. 5. The photometric magnitudes averaged over all the images for a particular exposure time. The photometry is consistent in all the exposures, which suggests that the effect of shutter speed is not significant. However, the photometric accuracy in the shortest exposures (<1 sec) is >0.015 magnitudes, so this effect can be investigated in more detail in a future program where we plan to observe bright and faint stars together to have high S/N both in short as well as long exposures.

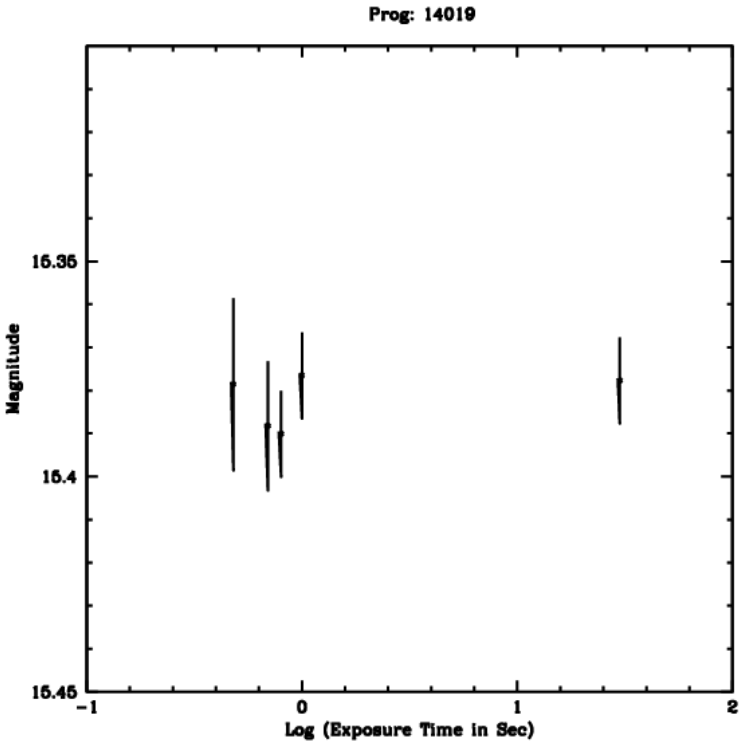

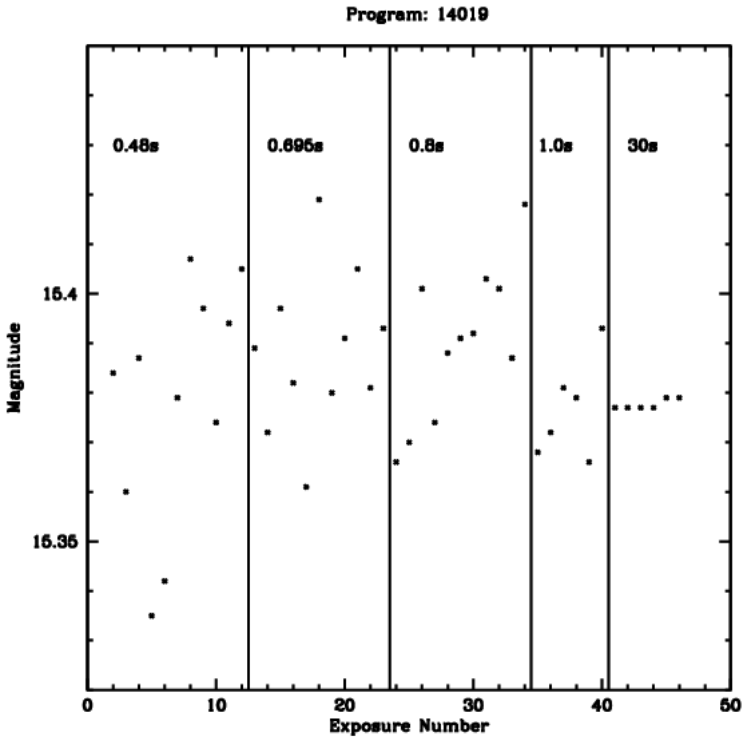

Fig. 6. The photometry for different exposure times are shown in separate bins. This shows that the photometry is consistent in all exposure times.

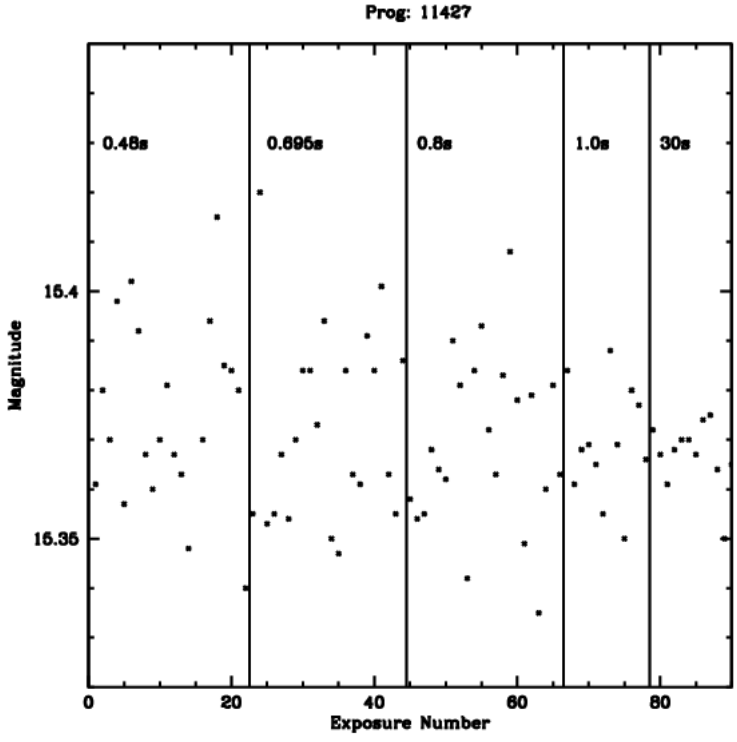

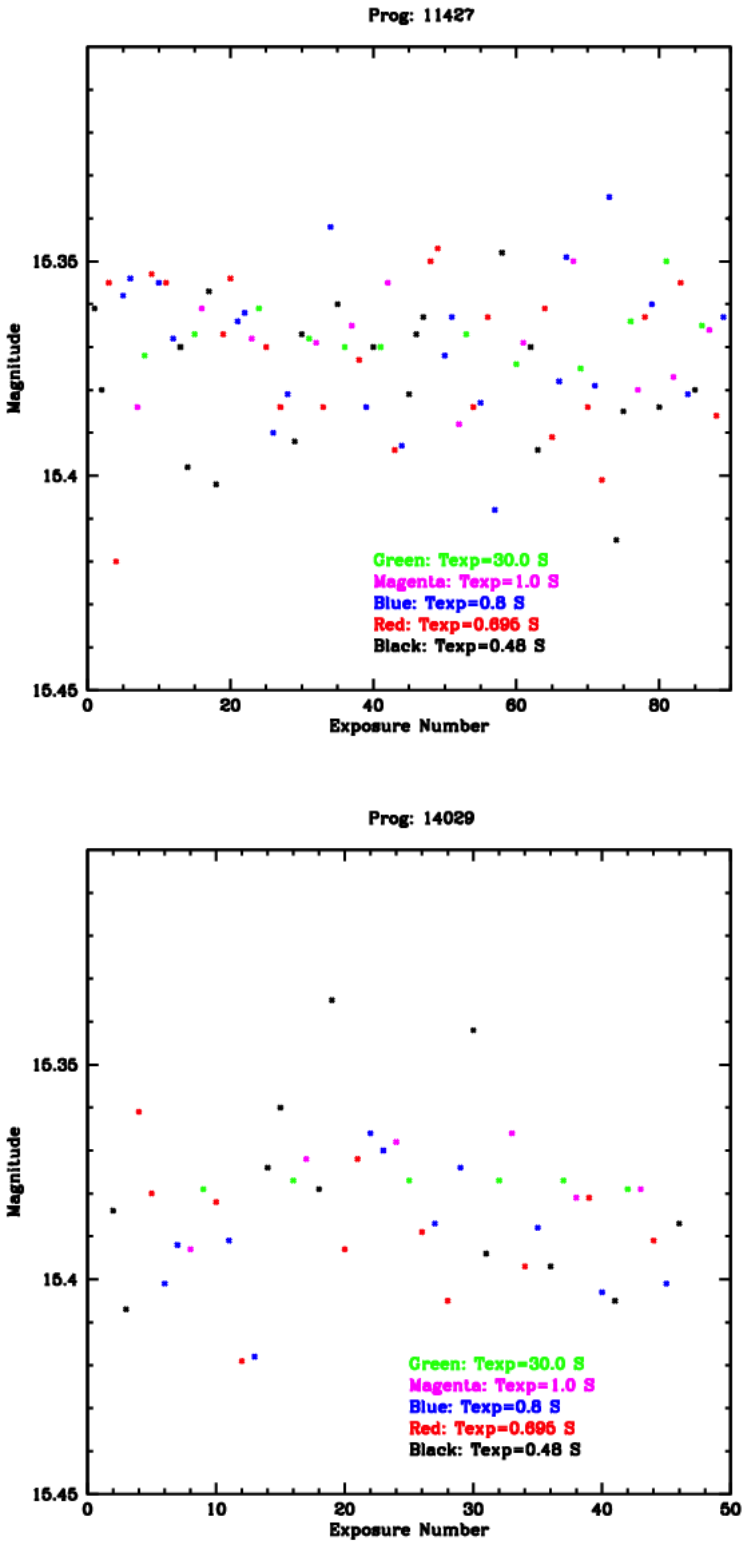

Fig. 7: The time sequence of the individual measurements for different exposure times are shown in different colors. Again, the photometry is consistent in all exposures, and does not show any time evolution, which confirms that the effect of shutter-speed is small.

Acknowledgements

We would like to thank Mike Fall for his prompt review and helpful comments.

References

Baggett, S. 2008, WFC3 ISR 2008-01

Bourque, M. & Baggett, S. WFC3 ISR 2013-09

Hartig, G, 2008, WFC3 ISR 2008-44

Dressel, L., 2014. "Wide Field Camera 3 Instrument Handbook, Version 6.0," section 2.3.3 (Baltimore: STScI)

Hilbert, B. 2009, WFC3 ISR 2009-25

Sahu, K, Baggett,S., and and MacKenty, J., 2014, WFC3 ISR 2014-09